EP 392: UG Project

Thermo-Optic analysis of metal-microheater integrated silicon waveguide phase-shifter

Department of Physics

Indian Institute of Technology (BHU), Varanasi

Supervisor: Dr. Rajeev Singh and Dr. Sunil K Singh

Sahil Singh

22174019

May 7, 2025

Contents

Thermo-Optic analysis of metal-microheater integrated silicon waveguide phase-shifter

Abstract: The following report presents a steady-state and transient thermal analysis of the Ti metal microheater integrated in Si waveguide followed by an analysis of associated optical loss and modulation characteristics of the simulated device, the workflow of the project is inspired primarily by work done in [4], Ramesh K. Gupta and Bijoy K. Das and [2], A. H. Atabaki et al.

---

1 Device architecture and numerical modeling

In reference to [4], two different architectures were designed categorized as Type 1 and Type 2, using similar design parameters and material properties (k,c,ρ) used in [2]. The temperature BC for the base of the Si substrate is set to 290 k. The ambient temperature is set at 300 K for the convection boundary condition, $-k\frac{\partial T}{\partial n} = h_{air}$ and the heat transport equation $\nabla.(-k\nabla T) + \rho c\frac{\partial T}{\partial t} = q_s$, with $q_s = 1.0mW$ is solved using the finite element method (FEM) in the lumerical HEAT solver [6].

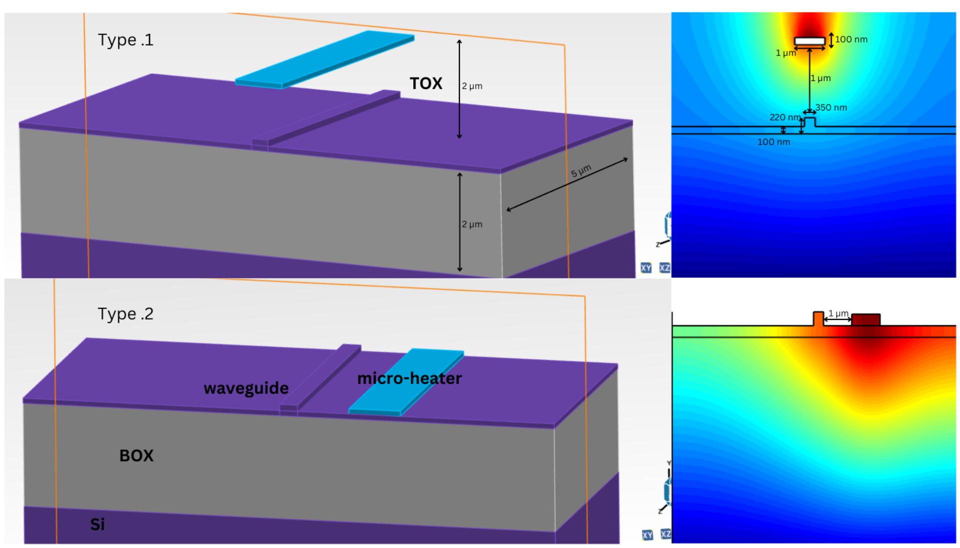

Figure 1: Type .1 architecture uses SiO2 as the top oxide (TOX) and type .2 is used for both air top and oxide cladding configuration, the corresponding side figures show the temperature distribution at SOI waveguide cross-section. The geometric parameters are set in such a way as to operate in TE_o polarized guided mode for $\lambda \in$ (1520nm,1630nm).

The "Thermal Analysis" section consists of steady state study of sensitivity parameter [4], $\Delta T_s = S_H.p_w$ and dependence of S_H on geometric parameters on the device, this is followed by transient evolution of temperature $\Delta T(t) = \Delta T_s(1 - e^{\frac{t}{\tau}})$, to estimate the value of τ in the SOI waveguide cross-section. The "Optical Analysis" section involves the numerical simulation of optical loss, introduced by the proximity of the metal microheater to the waveguide in the two architectures, using the lumerical MODE solver. At the end, in the Future Prospects section, I discuss my aspirations about the field.

2 Thermal Analysis

2.1 Steady State (Sensitivity S_H)

The steady-state temperature rise (ΔT_s) in the waveguide core is directly proportional to the Joule heating power consumption of the Ti metal microheater.The thermal sensitivity S_H of the phase shifter can be defined as:

$$\Delta T_s = S_H.p_w \tag{1}$$

where p_w is the Joule heating power consumption by the microheater per unit length. Further, the system's temperature rise ΔT_s is related to the power p_w by the conductance g_w (normalized by micro-heater length) of the system as $p_w = g_w.\Delta T_s$ giving the relation $g_w.S_H = 1$. Fig 2 shows the plot of ΔT_s vs p_w using data collected through numerical simulation of the heat transport equation.

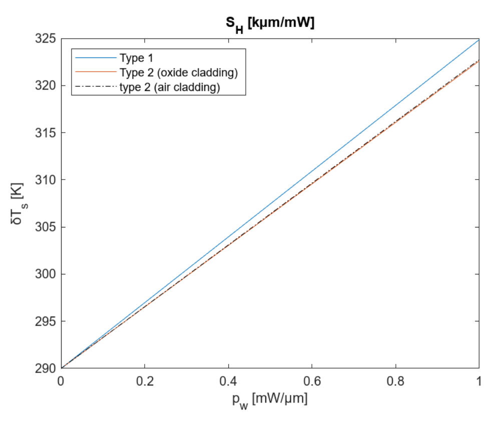

Figure 2: Given that $g_w.S_H = 1$, it can be explained that the Type.2 profile should have lower sensitivity due to higher conductance of the Si waveguide than the SiO2 cladding in Type.1 also due to slightly lower g_w of air the S_H of Type.2 air is more than Type.2 oxide cladding.

A more detailed simulation result for S_H parameter is shown in Figure 3 as a function of rib width (h) and waveguide-micro heater gap (d).

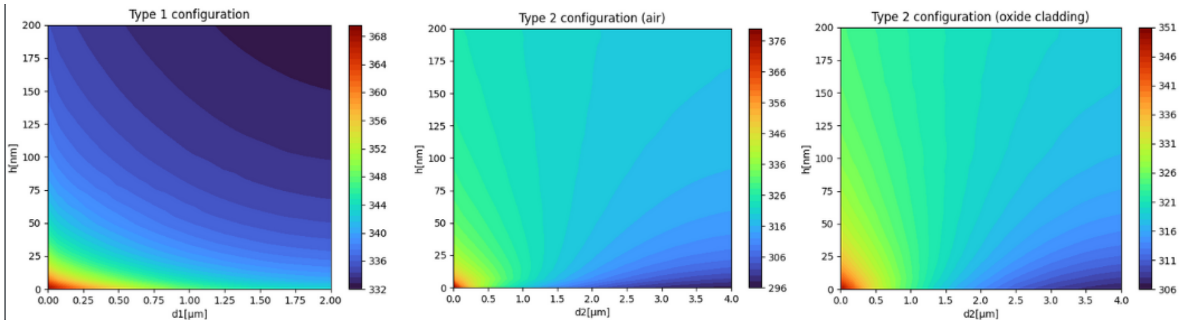

Figure 3: The contour plots for sensitivity S_H [Kμm/mW], calculated using Lumerical HEAT solver for TE_0 guided mode in the waveguide with H=220nm, Width=350nm, $\lambda = 1550nm$.

We see that for a given rib height 'h', we can increase the sensitivity by reducing 'd', but that will couple the evanescent tail of the guided mode into the metallic heater, leading to losses. These loss calculations were also simulated using the lumerical MODE solver and the results are shown in Figure 5.

2.2 Transient Mode (Time constant τ)

The theoretical evolution of the temperature inside the SOI waveguide core is given by.

$$\Delta T(t) = \Delta T_s * (1 - e^{\frac{t}{\tau}}) \tag{2}$$

where τ is the system's time constant, represented thermodynamically as $\tau = h_w/g_w$, h_w is the normalized heat capacitance of the system. Figure 4 shows the normalized temperature evolution profile and the estimated time constant.

The transient profile was calculated for 'd'$= 1\mu$m and 'h'$=$ 100nm using the lumerical HEAT solver, due to the higher conductivity of the air top and Si base of Type.2 architecture, the time constant comes out to be significantly lower as expected.

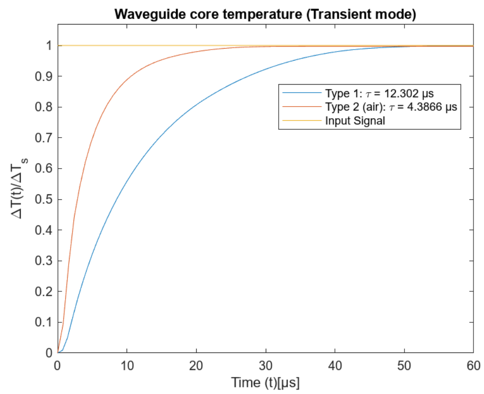

Figure 4: transient temperature rise $\Delta T(t)$ normalized to ΔT_s as a function time for a unit step-function excitation of input voltage signal to the microheaters.

3 Optical Loss

The proximity of metal microheater to the waveguide introduces optical attenuation of the guided mode because of the coupling of its evanescent tail with the metal microheater [1]. The optical loss coefficient α_h was numerically estimated using lumerical MODE solver, for TE_o guided mode as a function of "d" considering "h" (rib thickness) as a parameter, and the complex refractive index of Ti strip at $\lambda = 1550nm$. α_h

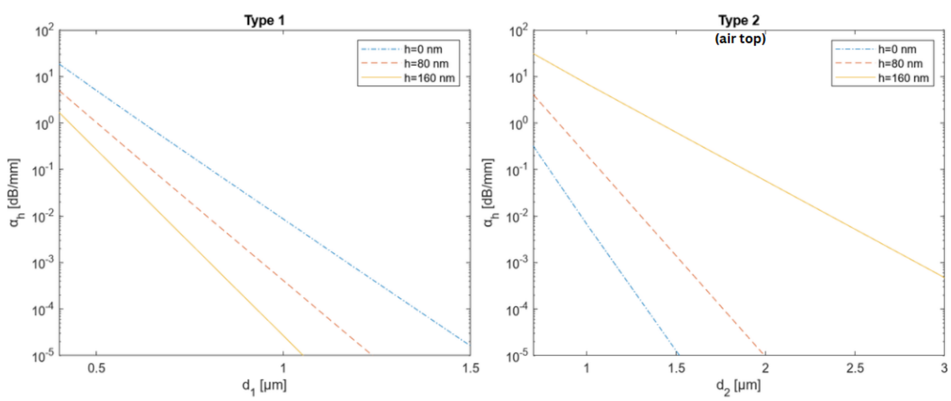

Figure 5: Numerical calculations were done for Ti micro heater strip of $w_h = 1\mu m$ and thickness $t_h = 100nm$. Refractive index of Ti at $\lambda = 1550nm$ is set to 3.6848+j4.6088.

(expressed in dB/mm) increases as the value of "d" decreases due to coupling of the evanescent tail with the metal strip. An opposite trend is observed for both architectures, in Type.1 (for a given 'd'), as h increases the strength of the evanescent tail in the y direction decreases so α_h reduces but for Type.2 as h increases α_h also increases due to poorer confinement of the guided mode, nevertheless α_h is always small enough ($\leq 0.1dB/mm$) for d $> 0.5\mu m$ and h=100nm.

The effect of material type and relative geometries of the waveguide and the metal-microheater is important to calculate the loss factor α_H. These parameters are important, especially when considering complex circuits involving multiple phase shifters, as this report proposes, since such circuits would require minimum crosstalk between individual phase shifters for maximum efficiency of information processing.

4 Future Prospects

The simulation data collected from lumerical MODE and HEAT solvers can be imported to lumerical INTERCONNECT to create a custom module [3].

Such modulators form the fundamental building block of more complex modulator networks (mesh fabrics) used in Programmable Photonic Circuits [5], such as the field programmable photonic gate arrays (FPPGA), which complement FPGAs in electronic integrated circuits. Owing to their improved performance against electronic integrated circuits, these PICs have huge commercial and research potential that can be explored in the coming decades.

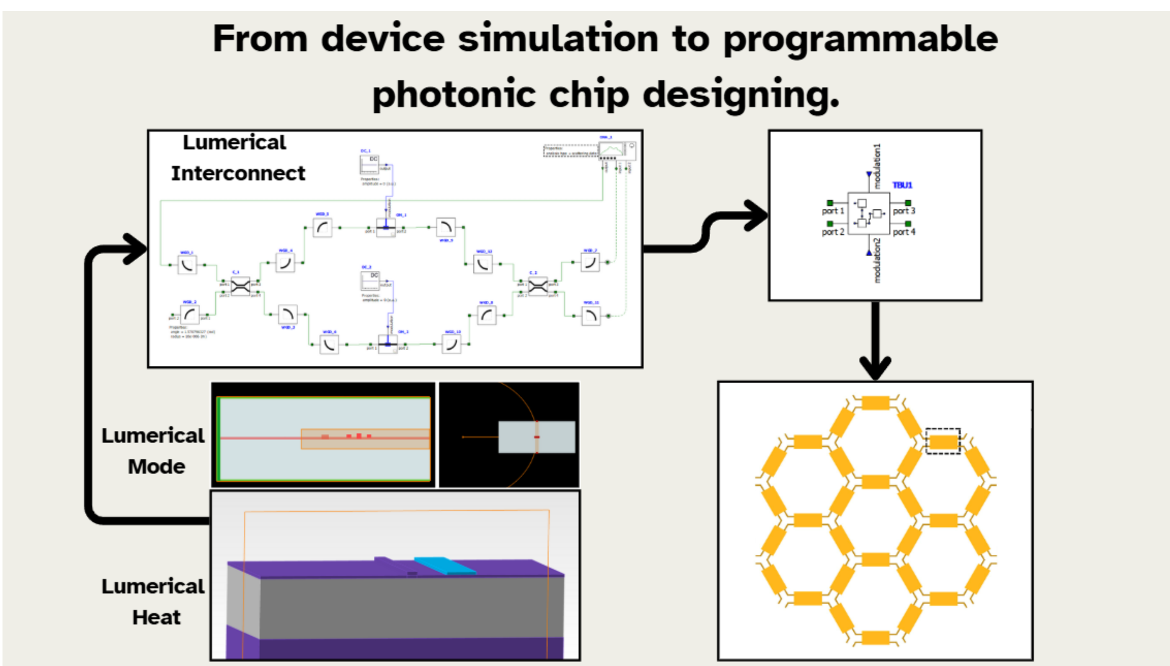

Figure 6: Workflow for PIC chip manufacturing [3]

Github link for my Lumerical scripts, models, and plots:-

https://github.com/tincan1596/analysis-of-integrated-metal-micro-heater-in-silicon-photonics.

5 Bibliography

References

[1] A. Yariv and A. P. Yeh. *Photonics: Optical Electronics in Modern Communications 6e*. Edition, Oxford University Press, 2007.

[2] A. H. Atabaki et al. "Optimization of metallic microheaters for high-speed reconfigurable silicon photonics". In: *Opt. Express* 18.17 (Aug. 2010), pp. 18312–18323. DOI: 10.1364/OE.18.018312. URL: https://opg.optica.org/oe/abstract.cfm?URI=oe-18-17-18312.

[3] Lukas Chrostowski and Michael Hochberg. *Silicon Photonics Design– From Devices to Systems*. Cambridge Press, 2015.

[4] Ramesh K. Gupta and Bijoy K. Das. "Performance analysis of metal-microheater integrated silicon waveguide phase-shifters". In: *OSA Continuum* 1.2 (Oct. 2018), pp. 703–714. DOI: 10.1364/OSAC.1.000703. URL: https://opg.optica.org/osac/abstract.cfm?URI=osac-1-2-703.

[5] Bogaerts et al. "Programmable photonic circuits". In: *Nature* (2020). DOI: 10.1038/s41586-020-2764-0. URL: https://www.nature.com/articles/s41586-020-2764-0.

[6] Ansys Lumerical inc. *Multiphysics and Lumerical solver*. Tech. rep.